



ELSEVIER

Thermochimica Acta 325 (1999) 143–149

thermochimica
acta

Irreversible thermal denaturation of lipase B from *Candida rugosa*

Valery L. Shnyrov^{1,a,*}, Luis Diez Martínez^b, Manuel G. Roig^b, Arkady E. Lyubarev^c,
Boris I. Kurganov^c, Enrique Villar^a

^a *Departamento de Bioquímica y Biología Molecular, Universidad de Salamanca, Plaza de los Doctores de la Reina, s/n, 37007 Salamanca, Spain*

^b *Departamento de Química Física, Facultad de Química, Universidad de Salamanca, Plaza de la Merced s/n, 37008 Salamanca, Spain*

^c *Bach Institute of Biochemistry, Russian Academy of Sciences, Leninsky pr. 33, 117071 Moscow, Russia*

Received 4 June 1998; accepted 12 October 1998

Abstract

The thermal denaturation of lipase B from *Candida rugosa* was studied by intrinsic fluorescence measurement, enzyme assay and differential scanning calorimetry. The calorimetric transitions for the enzyme were irreversible and strongly dependent on the scan rate, suggesting that the denaturation is under kinetic control. It is shown that this process can be interpreted in terms of a two-state first-order kinetic mechanism, although this interpretation is not very accurate. The energy of activation for first-order denaturation kinetics calculated by different methods is ca. 260 kJ/mol. © 1999 Elsevier Science B.V. All rights reserved.

Keywords: Irreversible thermal denaturation; Differential scanning calorimetry; Intrinsic fluorescence; Lipase B

1. Introduction

Triacylglycerol hydrolases (EC 3.1.1.3), or lipases, catalyse the reversible hydrolysis of tri-, di-, and monoglycerides and a variety of compounds containing carboxylic ester moieties that are not acylglycerols [1]. The potential of lipases in biotechnology is being increasingly recognised [2,3], mainly due to their availability and stability. This is especially the case of extracellular lipases from microorganisms.

Owing to the high activity of the lipase from *Candida rugosa* in hydrolysis [4], as well as in synthesis [5], it is becoming one of the most widely used enzymes in industry. This lipase is a single-domain molecule and belongs to the family of α/β hydrolase fold proteins [6] with ten strands of a large β -sheet and three strands of a small β -sheet interconnected by α -helices [7]. As inferred from sequence alignments, the catalytic triad is formed by Ser 209, His 449 and Glu 341 [7], Ser 209 being embedded in the characteristic super-secondary structural motif – the strand-turn-helix – found in all other lipases [8–10].

Among the closely related lipase isoforms from *Candida rugosa*, two major populations, called lipases A and B, have been purified [11–13]. Both lipases

*Corresponding author. Tel.: +34-23-294-465; fax: +34-23-294-579; e-mail: shnyrov@gugu.usal.es

¹Permanent address: Institute of Theoretical and Experimental Biophysics, Russian Academy of Sciences, 142292 Pushchino, Moscow region, Russia.

have similar amino acid contents, *N*-terminal sequences and molecular weights close to 60 kDa, but they differ in their neutral sugar contents and hydrophobicity, the presence of isoforms in lipase B as observed by electrofocusing, their stability with regards to pH and temperature, and their substrate specificity [13].

The biological functions of proteins depend on the correct folding of their native structure. Loss of this folded structure leads to an unfolded, inactive state. Consequently, a better understanding of the mechanisms of protein denaturation is of great interest from both, the theoretical and practical points of view.

Differential scanning calorimetry (DSC) is currently the most useful technique for characterising the thermal stability of proteins [14], quantitatively defined as the Gibbs energy of unfolding [15]. Thermodynamic analysis of DSC data on proteins requires that denaturation should be a reversible equilibrium process [16]. Nevertheless, it is well known that the thermal denaturation of most proteins is calorimetrically irreversible and also strongly dependent on the scan rate. And if the DSC transitions corresponding to irreversible protein denaturation are highly scan-rate dependent, it is clear that the overall denaturation process is controlled kinetically. Therefore, analysis of the DSC curves in equilibrium thermodynamics should be ruled out [17].

In this paper, we describe the thermal denaturation of lipase B from *Candida rugosa* as studied by the DSC method, intrinsic fluorescence experiments, and enzymatic activity assays. The thermal unfolding of lipase B was found to be irreversible and scan-rate dependent and we, therefore, analysed this non-equilibrium process based on kinetic models.

2. Materials and methods

Lipase type VII, *p*-nitrophenyl acetate (*p*-NPC2), tributyrin (99%) and HEPES were from Sigma (St. Louis, MO). Phenyl-Sepharose CL-4 was from Pharmacia (Sweden). The kit of chemicals for protein concentration determinations was from the Bio-Rad Laboratories (Richmond, CA). *p*-Nitrophenol, acetic acid, NaOH, NaCl, HCl were from Merck (Darmstadt, Germany) and the other reagents from Panreac (Barcelona, Spain).

All reagents were of the highest purity available. Double-distilled water was used throughout.

The isoenzyme lipase B from *Candida rugosa* was purified from lipase type VII, which is supplied in the lyophilised form containing 30% lactose and a specific activity of 700–1500 units/(mg of solid) using emulsified olive oil at pH 7.2 as substrate. Purification was performed in accordance with [18]. The separation procedure is based on a single step of hydrophobic chromatography in Phenyl-Sepharose CL-4 matrix and subsequent elution with 1-mM sodium phosphate buffer, pH 7.0. Lipase B was further purified by Sephacryl HR 100 chromatography. The purity of the enzyme was ca. 95% as checked by SDS/PAGE [19].

Unless otherwise indicated, all the experiments were carried out in 10 mM HEPES buffer, pH 7.2 (buffer A).

Protein concentrations were determined by the method of Lowry et al. [20].

The pure lipase B solution was finally dialysed overnight in a large volume of buffer A before use.

Fluorescence measurements were performed on a Hitachi F-4010 spectrofluorimeter. Excitation at 280 nm (with excitation and emission slit widths of 5 nm) was used because the contribution of tyrosine to the intrinsic fluorescence spectrum of lipase B was small. For the sake of convenience, spectra were analysed directly without further correction. The position of the middle of a chord, drawn at the 80% level of maximum intensity, was taken as the position of the emission maximum (λ_{max}). Fluorescence spectra were analysed on the basis of the model of discrete states of tryptophan (see, for details, Ref. [21]). The temperature dependence of the fluorescence spectrum characteristics was investigated using thermostatically-controlled water circulating in a hollow brass cell-holder. The temperature in the sample cell was monitored with a thermocouple immersed in the cell under observation. To study the kinetics of heat denaturation by intrinsic fluorescence, 0.01 ml samples of a 0.14-mM lipase B solution were added to 2 ml of buffer A previously thermostatted at the desired temperature in the fluorimeter cuvette. The mixture was stirred constantly in the cuvette and an emission spectrum of lipase B was recorded at a certain time interval. In all experiments, the time for temperature equilibrium in the cuvette after sample introduction did not exceed 5 s.

Lipase activity was assayed following the hydrolysis of tributyrin in a Radiometer pH-stat at 303 K in 1 mM Tris-HCl, pH 7.2 and esterase activity, using *p*-NPC2 as substrate, was followed spectrophotometrically at 303 K on a Beckman DU-7 spectrophotometer, equipped with magnetic stirring as described in Ref. [13].

DSC experiments were performed on a MicroCal MC-2 differential scanning microcalorimeter (MicroCal, Northampton, MA) with cell volumes of 1.22 ml, interfaced with a personal computer (IBM-compatible). Different scan rates within the 0.212–1.45 K/min range were employed. Before measurement, samples were degassed with stirring in an evacuated chamber for 5 min at room temperature and then immediately loaded into the calorimeter cell. The final dialysis buffer (also degassed) was loaded into the reference cell. A pressure of 2 atm of dry nitrogen was always kept over the liquids in the cells throughout the scans to prevent any degassing during heating. A background scan collected with a buffer in both cells was subtracted from each scan. The reversibility of the thermal transitions was checked by examining the reproducibility of the calorimetric trace in a second heating of the sample immediately after cooling from the first scan. The experimental calorimetric traces were corrected for the effect of instrument response time using the procedure described previously [22].

The excess molar heat capacity was calculated assuming the molecular mass of lipase B to be 60 kDa.

The temperature-dependence of the molar heat capacity of lipase B was further analysed and plotted using the Windows-based software package (Origin) supplied by MicroCal.

Kinetic analysis of the DSC curves was carried out according to models elaborated as approximations to the whole Lumry–Eyring model [23–25]. To fit the theoretical curves to the experimental data, we used an original programme developed for IBM-compatible computers by A.E. Lyubarev [23,24].

The correlation coefficient (r), used as a criterion for fitting accuracy, was calculated according to the equation:

$$r = \sqrt{1 - \frac{\sum_{i=1}^n (y_i - y_i^{\text{calc}})^2}{\sum_{i=1}^n (y_i - y_i^{\text{m}})^2}} \quad (1)$$

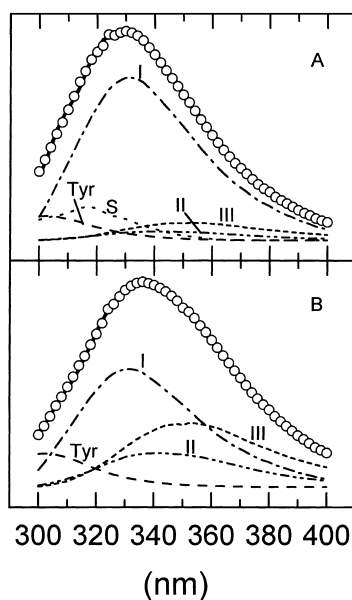


Fig. 1. Fitting of the experimental fluorescence spectra of intact (A) and thermally-denatured (B) lipase B (O) by theoretical spectra (thick solid lines), which are the sums of the spectral components: tyrosine (Tyr), S, I, II and III (thin interrupted lines).

where y_i and y_i^{calc} are, respectively, the experimental and calculated values of C_p^{ex} ; y_i^{m} the mean of the experimental values of C_p^{ex} and n the number of points.

3. Results and discussion

Fig. 1 (solid lines) shows the fluorescence spectra of intact and thermally denatured lipase B excited at 280 nm. Excitation at 297 nm gave almost identical spectra. According to the model of discrete states of tryptophan residues in proteins (see, for details, Ref. [21]), there are several most probable physical states for tryptophan residues. Each state is characterised by its fluorescence spectrum. Analysis of the emission spectra of intact lipase B (Fig. 1(A)) on the basis of the model of discrete states of tryptophan residues shows that they can be fitted by four spectral components, two of which (forms S (ca. 10%) and I (ca. 75%)) are due to the emission of buried tryptophans in a polar environment (spectral form S corresponds to the emission of the indole chromophore located inside the protein globule and forming a 1:1 exciplex with some neighbouring polar protein group while spectral

form I corresponds to the emission of chromophore forming a 2 : 1 exciplex in the same environment). The others (form II (ca. 5%) and form III (ca. 10%)) are due to the emission of tryptophans located at the protein surface (spectral form II corresponds to the emission of the chromophore which is in contact with bound water while spectral form III corresponds to the emission of the chromophore which is in contact with free water molecules).

Complete heat denaturation of lipase B (Fig. 1(B)) results in the disappearance of component S and a decrease in the contribution of component I (ca. 50%). In this case, components II (ca. 17%) and III (ca. 33%) contribute strongly to the total emission spectrum.

In view of these results, we used the changes in some parameters of the fluorescence spectra to analyse the effect of temperature on the kinetics of lipase B denaturation. Fig. 2 shows the data on lipase B denaturation as monitored by changes in the fluorescence quantum yield in relative units (A), as well as the position of the emission maximum (B) obtained at the following four temperatures: 324, 327, 329 and 331 K. Fig. 2(B) shows that, although the denaturation rate does increase with temperature, the final level of intrinsic fluorescence is independent of the denaturation temperature. This strongly suggests that the thermal denaturation of lipase B may not actually be a reversible equilibrium between the native and denatured enzyme because, if this were the case, the relative amounts of native and denatured states would be expected to show a definite temperature dependence. Therefore, this appears to be a kinetic phenomenon involving an irreversible process. The best fit of the experimental data represented as dashed lines in Fig. 2 was achieved with an exponential function:

$$F + F_{\infty} + (F_0 - F_{\infty})\exp(kt) \quad (2)$$

where F is function value at a given time (t) and F_0 and F_{∞} are normalisation parameters (at $t=0$, $F=F_0+F_{\infty}$, and at $t=\infty$, $F=F_{\infty}$), indicating a first-order kinetic process:

$$N \xrightarrow{k} D \quad (3)$$

The values of the rate constant k derived from these fittings hardly changed at all with protein concentrations within the 0.1–1 mg/ml range. The temperature

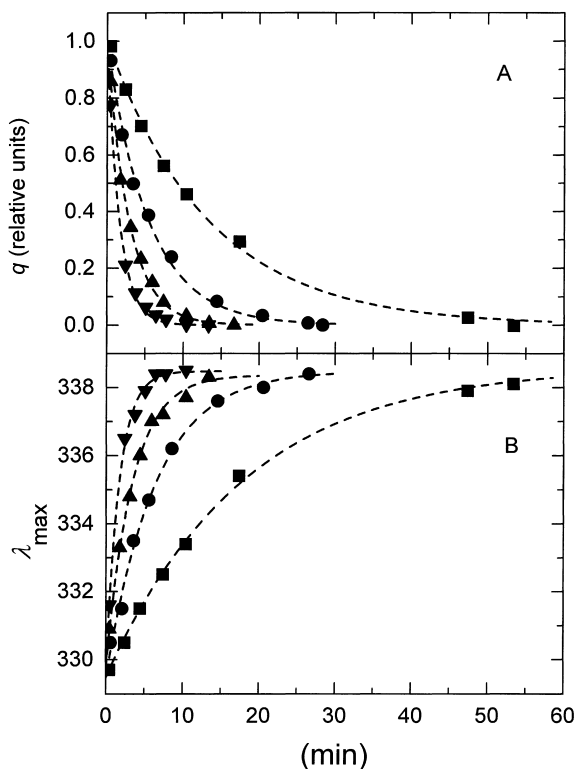


Fig. 2. Effect of temperature on the kinetics of the thermal denaturation of lipase B in buffer A as monitored by intrinsic fluorescence. Symbols refer to the experimental data at temperatures of 324 K (squares), 327 K (circles), 329 K (triangles) and 331 K (inverted triangles). (A) normalized changes in the fluorescence quantum yield; and (B) changes in the position of the emission maximum. Dashed lines represent the best fit to the first-order kinetic process (Eq. (2)).

dependence of the rate constant can be expressed by the Arrhenius equation:

$$k = \exp \left[\frac{E_A}{R} \left(\frac{1}{T^*} - \frac{1}{T} \right) \right] \quad (4)$$

where E_A is the energy of activation for the denaturation process and T^* the temperature at which k is equal to 1 min^{-1} . The energy of activation was deduced from the Arrhenius plot of $\ln k$ vs. $1/T$, represented in Fig. 3. A good coincidence for different fluorescence parameter changes is seen. The E_A value of $276.5 \pm 5.9 \text{ kJ/mol}$ was obtained from the slope of this Arrhenius plot.

In the next experiments, samples of lipase B were heated up to defined temperatures at a scan rate of ca.

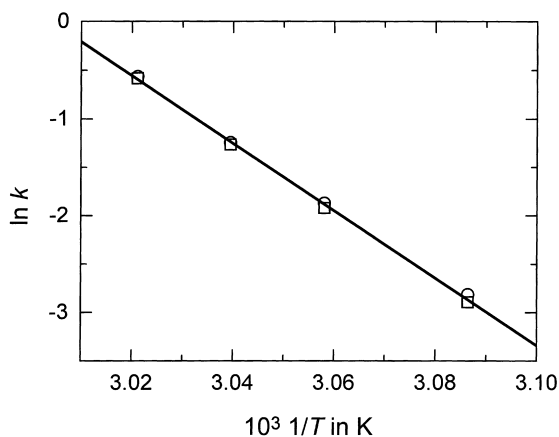


Fig. 3. Dependence of the logarithm of the inactivation rate constant (min^{-1}) on the reciprocal value of the absolute temperature as monitored by intrinsic fluorescence. (○), Fluorescence quantum yield; and (□), position of emission maximum.

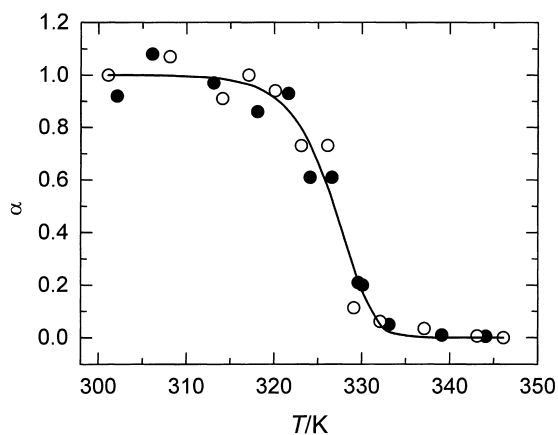


Fig. 4. Temperature dependence of lipase (●) and esterase (○) activities (scan rate 25 K/h); (—), the best fit using Eq. (5).

25 K/h. The samples were then immediately cooled and lipase and esterase activities were determined as described in Section 2. The changes in both the lipase B activities with temperature (symbols in Fig. 4) show that a concomitant loss of enzymatic activities occurs in the 323–328 K region. Taking into account the kinetic character of lipase B denaturation, we fitted these data to Eq. (5) which is valid for model (3):

$$\alpha = \exp \left\{ -\frac{1}{v} \int_{T_0}^T \exp \left[\frac{E_A}{R} \left(\frac{1}{T^*} - \frac{1}{T} \right) \right] dT \right\} \quad (5)$$

where α refers to the folded fraction [26]. This fitting afforded the T^* parameter and the activation energy for lipase B. These were 335.7 ± 1.5 K and 256.9 ± 11 kJ/mol, respectively.

To obtain a more accurate information about the mechanism of thermal denaturation of lipase B from *Candida rugosa*, we carried out DSC experiments in buffer A. The DSC transitions of lipase B were calorimetrically irreversible since no thermal effect was observed in a second heating of the lipase B solution. Fig. 5 (symbols) shows the effect of the scan rate on the DSC transitions corresponding to the thermal denaturation of lipase B. These transitions have previously been corrected for the effect of the slow time response of the calorimeter [22]. From the strong effect of the scan rate observed, it can be deduced that the thermal denaturation of lipase B is at least partly under kinetic control. Therefore, to analyse the calorimetric profiles obtained we used some models of irreversible protein denaturation.

The simplest model of irreversible denaturation is model (3). This model was investigated in regard to its applications to DSC data by Sanchez-Ruiz et al. [17,23,27,28]. The equation that quantitatively explains the thermal capacity curves (C_p^{ex}) as a func-

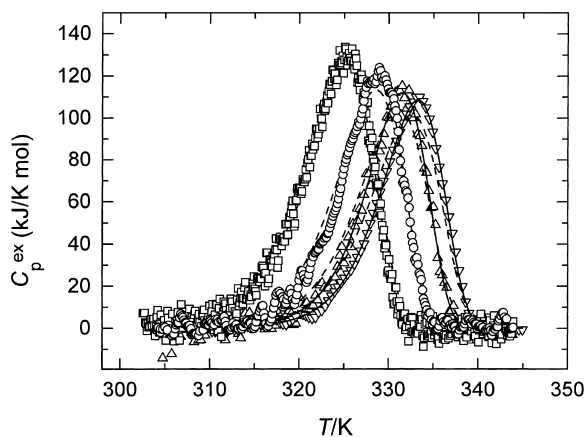


Fig. 5. Calorimetric profiles obtained for lipase B in buffer A at scan rates of 0.212 (squares), 0.493 (circles), 0.99 (triangles) and 1.45 (inverted triangles) K/min; solid lines are the best fits by using Eq. (6) to each experimental curve; dashed lines are the best fit using Eq. (6) simultaneously on all curves.

tion of absolute temperature (T) at a constant scan rate of $v=dT/dt$ (K/min) is as follows [23]:

$$C_p^{\text{ex}} = \frac{1}{v} Q_t \exp \left\{ \frac{E_A}{R} \left(\frac{1}{T^*} - \frac{1}{T} \right) \right\} \times \exp \left\{ -\frac{1}{v} \int_{T_0}^T \exp \left[\frac{E_A}{R} \left(\frac{1}{T^*} - \frac{1}{T} \right) \right] dT \right\} \quad (6)$$

where Q_t is the total heat of the denaturation process (proportional to the area below the measured curve).

The results of fitting of Eq. (6) to the experimental data are shown in Fig. 5 (solid and dashed lines) and in Table 1. When fitting was carried out on the individual experimental curves separately, good approximation was achieved (solid lines). However, as can be seen from the table, the parameter estimates vary with the different scan rate. When we carried out fitting simultaneously on all the curves, fitting accuracy was low (Fig. 5, dashed lines, and Table 1, right-hand column).

Previously, we had proposed some criteria for the validity of model (3) [23], one of them to plot the values of $\ln [vC_p^{\text{ex}}/(Q_t - Q)]$ vs. $1/T$. If the data satisfy the model, the experimental points corresponding to all the scan rates should lie on a common straight line.

Fig. 6 shows the DSC data for lipase B in the above-mentioned coordinates. As can be seen from the plot, lines corresponding to different scan rates diverge. It may thus be concluded that the thermal denaturation of lipase B can only be described approximately by the one-step model (3).

We next attempted to analyse the DSC data for lipase B using two two-step irreversible models, as previously described [24]. These were the Lumry–Eyring model, with a fast equilibrating first step, and the model that includes two consecutive irreversible steps. When fitting was carried out on the individual

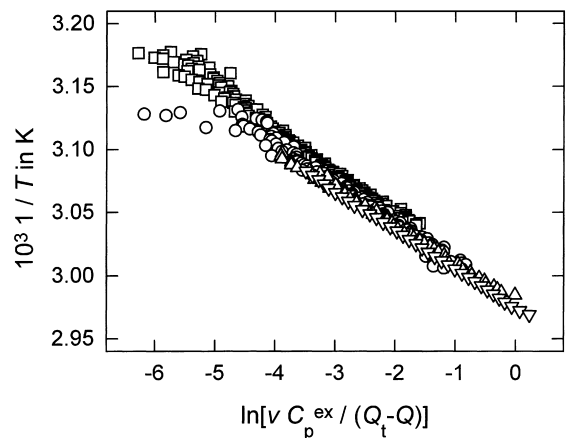


Fig. 6. Dependences of $\ln[vC_p^{\text{ex}}/(Q_t - Q)]$ on $1/T$ for lipase B calculated from the experimental data shown in Fig. 5.

experimental curves separately, the parameter estimates varied with the different scan rates to a greater extent than when model (3) was used. When we carried out fitting simultaneously on all the curves, fitting accuracy was not high.

In the next experiment, we heated the enzyme to 324.3 K with a scan rate of 59.5 K/h; we then cooled it to 288 K and reheated it with the same scan rate. Fig. 7 shows the reheating scan in a comparison with the full scan at this scan rate. The curves may be seen to differ only by a scale factor determined by a difference in the amount of protein undergoing denaturation. If the model including two consecutive irreversible steps would be valid, according to our calculations with the parameters providing the best fit simultaneously to all the curves, a reheating scan should be higher in the initial part than the original scan (data not shown). It may, therefore, be concluded that this model is not valid for the thermal denaturation of lipase B.

To conclude, it may be seen that there is a reasonable agreement between the parameters obtained with

Table 1
Arrhenius equation parameter estimates for the one-step model of thermal denaturation of lipase B

Parameter	Temperature scan rate/ (K/min)				Fitting to all curves
	0.212	0.493	0.99	1.45	
Q_t (kJ/mol)	1248±8	1067±12	997±8	996±4	
T^* K	336.0±0.13	335.3±0.13	335.7±0.07	336.3±0.03	335.3±0.06
E_A (kJ/mol)	241.4±2.1	272.0±3.8	275.3±2.5	268.6±1.3	239.3±1.3
r	0.988	0.982	0.995	0.999	0.983

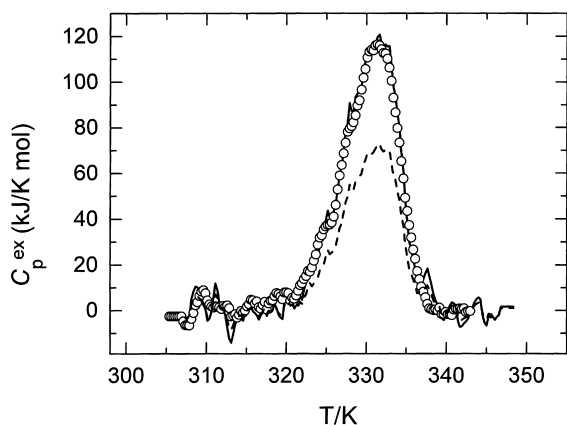


Fig. 7. Original and reheating scans for lipase B (scan rate 59.5 K/h). Symbols, original scan; (---), reheating after first heating to 324.3 K and cooling to 288 K; and (—), reheating scan multiplied by the ratio of calorimetric enthalpies for the original and reheating scans.

different methods used. Thus, the denaturation of the lipase B can be interpreted in terms of a two-state first-order kinetic mechanism although such a description is not very accurate. It is quite possible that some other processes might be involved and might distort the first-order kinetics.

Acknowledgements

We thank Dr. G.G. Zhadan for useful discussion. Thanks are also due to N.S.D. Skinner for proof-reading the manuscript. V.L. Shnyrov is a sabbatical leave recipient from the Spanish DGICYT (ref. SAB 95-0561).

References

- [1] R.G. Jensen, D.R. Galluzas, V.J. Bush, *Biocatal.* 3 (1990) 307.
- [2] F. Bjorkling, S.E. Godtfredsen, O. Kirk, *TIBTECH* 9 (1991) 360.
- [3] R.I. Kazlauskas, *TIBTECH* 11 (1993) 439.
- [4] L. Alberghina, R.D. Schmidt, R. Verger (Eds), *Lipases: Structure, Mechanism and Genetic Engineering*, VCH, Weinheim, 1991.
- [5] A. Mustranta, *Appl. Microbiol. Biotechnol.* 38 (1992) 61.
- [6] D. Ollis, E. Cheah, M. Cygler, B. Dijkstra, F. Frolow, S.M. Franken, M. Harel, S.J. Remington, I. Silman, J.D. Schrag, J.L. Sussman, K.H.G. Verscheuren, A. Goldman, *Protein Eng.* 5 (1992) 197.
- [7] P. Grochulski, Y. Li, J.D. Schrag, F. Bouthillier, P. Smith, D. Harrison, B. Rubin, M. Cygler, *J. Biol. Chem.* 268 (1993) 12843.
- [8] L. Brady, A.M. Brzozowski, Z.S. Derewenda, E. Dodson, G. Dodson, S. Tolley, J.P. Turkenburg, L. Christiansen, B. Huge-Jensen, L. Norskov, L. Thim, U. Menge, *Nature* 343 (1990) 767.
- [9] F.K. Winkler, A. D'Arcy, W. Hunziker, *Nature* 343 (1990) 771.
- [10] J.D. Schrag, Y. Li, S. Wu, M. Cygler, *Nature* 351 (1991) 671.
- [11] K. Veeraragavan, B.F. Gibbs, *Biotechnol. Lett.* 11 (1989) 345.
- [12] M. Brahimi-Horn, M.L. Guglielmino, L. Elling, L.G. Sparrow, *Biochim. Biophys. Acta* 1042 (1990) 51.
- [13] M.L. Rúa, T. Diaz-Mauriño, V.M. Fernández, C. Otero, A. Ballesteros, *Biochim. Biophys. Acta* 1156 (1993) 181.
- [14] V.L. Shnyrov, J.M. Sanchez-Ruiz, B.N. Boiko, G.G. Zhadan, E.A. Permyakov, *Thermochim. Acta* 302 (1997) 165.
- [15] W.J. Becktel, J.A. Schellman, *Biopolym.* 26 (1987) 1859.
- [16] P.L. Privalov, *Adv. Protein Chem.* 35 (1982) 1.
- [17] E. Freire, W.W. van Osdol, O.L. Mayorga, J.M. Sanchez-Ruiz, *Ann. Rev. Biophys. Chem.* 19 (1990) 159.
- [18] M.L. Rúa, A. Ballesteros, International patent PCT/ES93/00058, (1993).
- [19] U.K. Laemmli, *Nature* 227 (1970) 681.
- [20] O.H. Lowry, N.I. Rosenbrough, A.L. Farr, R.J. Randall, *J. Biol. Chem.* 193 (1951) 265.
- [21] E.A. Permyakov, *Luminescence Spectroscopy of Proteins*, CRC Press, Boca Raton, FL, 1993.
- [22] O. López-Mayorga, E. Freire, *Biophys. Chem.* 87 (1987) 87.
- [23] B.I. Kurganov, A.E. Lyubarev, J.M. Sánchez-Ruiz, V.L. Shnyrov, *Biophys. Chem.* 69 (1997) 125.
- [24] A.E. Lyubarev, B.I. Kurganov, A.A. Burlakova, V.N. Orlov, *Biophys. Chem.* 70 (1997) 247.
- [25] D. Milardi, C. La Rosa, D. Grasso, *Biophys. Chem.* 52 (1994) 183.
- [26] P.E. Morin, D. Diggs, E. Freire, *Biochem.* 29 (1990) 781.
- [27] J.M. Sánchez-Ruiz, J.L. Lopez-Lacomba, M. Cortijo, P.L. Mateo, *Biochem.* 27 (1988) 1648.
- [28] J.M. Sánchez-Ruiz, *Subcell. Biochem.* 24 (1995) 133.